Catalysis Today xxx (2015) xxx–xxx

Contents lists available at ScienceDirect

Catalysis Today

journal homepage: www.elsevier.com/locate/cattod

Experimental design optimization of the tetralin hydrogenation over Ir–Pt-SBA-15

Verónica A. Valles, Brenda C. Ledesma, Lorena P. Rivoira, Jorgelina Cussa, Oscar A. Anunziata, Andrea R. Beltramone *

Centro de Investigación en Nanociencia y Nanotecnología (NANOTEC), Facultad Regional Córdoba, Universidad Tecnológica Nacional, Maestro López y Cruz Roja Argentina, 5016 Córdoba, Argentina

ARTICLE INFO

Article history:
Received 2 April 2015
Received in revised form 3 July 2015
Accepted 5 July 2015
Available online xxx

Keywords:
Iridium–platinum containing SBA-15
Tetralin hydrogenation
Trans/cis ratio
Experimental design

ABSTRACT

Experiment design-response surface methodology (RSM) is used in this work to model and optimize two responses in the hydrogenation of tetralin to decalin using bimetallic Ir–Pt-SBA-15 catalyst. In this study, we analyze the influence of the nature of the catalyst (metal molar fraction and metal loading), the catalyst/substrate ratio and the temperature of the reaction as factors for the design. The responses analyzed were conversion at 3 h and at 5 h of reaction time. The response surfaces were obtained with the Box–Behnken design, finding the best combination between the reaction parameters that allowed optimizing the process. By applying the statistic methodology, the higher levels of the two objective functions were obtained employing the catalyst with 1 wt.% of iridium and 0.7–0.8 wt.% of platinum; the optimal ratio between mass of catalyst and mole of tetralin was 17–19 g/mol and temperature between 200 and 220 °C.

1. Introduction

Supply and demand have generated the need to convert heavy crude oils that are richer in heteroatoms than traditional crudes. This fact requires improvement of the hydrotreating processes to meet the current and future fuel specifications [1–7]. Refineries are currently looking to increase cetane number and to limit aromatics in diesel fuel in order to improve combustion efficiency and reduce particulate matters, NOx emissions and SOx emissions. The cetane number is a measure of ignition quality and is indicative of the degree of combustion efficiency of the fuel, so that the maximum amount of usable energy occurs. Therefore, the cetane number is considered as a good parameter to evaluate the amount of emissions both solid and gaseous of diesel. In this case, the increase in cetane number may strongly depend on the nature of the crude used as well as blending strategies used by the refiners. In the last years, refineries have been using greater fractions of LCO (light cycle oil) in pools of diesel. The incorporation of these cuts with a high content of aromatics and low cetane number has a negative influence on the final cetane number of diesel.

The sulfur and nitrogen compounds found in synthetic feedstock and heavy petroleum fractions can strongly inhibit hydroprocessing reactions through competitive adsorption. The presence of these species even at low concentrations may limit the observed catalytic activity and necessitate the use of higher pressures and temperatures to obtain desired conversions. Therefore, the need of more active catalysts is crucial in this process. The development of highly active and selective hydrotreating catalysts is one of the most pressing problems facing the petroleum industry. As an alternative for NiMo catalyst, Usman et al. [8,9] presented a study of a highly selective and stable catalytic approach for producing tetralin, using transition metal phosphides (MoP, Ni_2P, Co_2P, and Fe_2P) supported on zeolites. The existence of weak, moderate, and Lewis acidic sites over MoP were responsible for its high tetralin selectivity and stability in a fixed-bed reactor. MoP/HY catalyst was found to be highly selective for tetralin during the naphthalene hydrogenation reaction. MoP/alumina possessed a moderate activity but its intrinsic property is six time higher than MoS_2 in HDN reactions according to Stinner et al. [10].

Noble metal-based catalysts are an interesting alternative, since they have high activity for hydrogenation of aromatic hydrocarbons, and the process can then perform at low temperatures and pressures. The metal function is usually provided by Pt and/or Pd but it has been shown that Ir, Ru and Rh also have exceptional activity and selectivity for the target reaction of hydrogenation [11–13]. It is known that Iridium o platinum catalyst are more expensive than NiMo catalyst, but it allow to work at lower temperatures and pressures due its higher activity, therefore, the cost of the catalyst

* Corresponding author.
E-mail address: abeltramone@scdt.frc.utn.edu.ar (A.R. Beltramone).

http://dx.doi.org/10.1016/j.cattod.2015.07.018
0920-5861/

are compensated with the saving in the operating conditions and the much higher activity.

In previous works [14–16] we demonstrate that Ir-modified mesoporous materials possesses a kinetic constant one order of magnitude higher than commercial NiMo catalysts. The catalytic results revealed the good performance of these monometallic Ir-modified catalysts at low temperatures, where high conversions and high yields of hydrogenation products were obtained, improving on the behavior displayed by the commercial catalyst. It is noteworthy that these catalysts need lower contact times and hydrogen/tetralin molar ratios than the NiMo catalyst, thus reducing the cost of the process if used in future industrial applications. As a result, Ir-catalysts supported on SBA-3 and SBA-16 modified with Al and especially Ti, were more resistant to N or S poisoning than their analogs pure silica-supported.

Hydrogenation can saturate a large amount of aromatic; however, the cetane number may still be lower than the target values specified in future diesel legislations. Therefore, the opening of at least one of the naphthenic rings is a promising reaction to attain high cetane number [17]. Dokjampa et al. [18] had shown that not every ring-opening path results in an increase in cetane number. Tetrahydronaphthalene (tetralin) has been frequently used to represent aromatics in diesel fuels in hydrogenation reactions [18–21], the two products of the hydrogenation of tetralin are cis- and trans-decalin. They have different reactivity in the subsequent ring-contraction and ring opening reactions [22]. They demonstrated that cis-decalin is more active toward ring opening, but trans-decalin is thermodynamically more stable. It was shown that the conversion of pure cis-decalin at moderate temperatures was more selective to C10 ring-opening products while the dominant products from trans-decalin were cracking products (C1–C9) [22–25]. In this context, Pt has been reported to be a very efficient metal for hydrogenation [26], while Ir has been recognized for its high activity in the hydrogenolysis reactions [27–30]. Currently, much attention has been paid to the bimetallic catalysts because they can combine two or more functions. The functionality of a catalyst may be due to active sites generated for supported metals and the interaction with the support [31–35].

The Pt–Pd catalysts have been extensively studied in order to improve the sulfur tolerance and catalytic activity. The starting point of these studies is the superior activity, selectivity and stability showed by these catalysts compared with monometallic Pt or Pd catalysts and has proven to have greater resistance to poisons compared to monometallic catalysts.

The mesoporous materials have been widely used in developing multifunctional catalysts for bringing large areas, where active metals can be deposited, giving good dispersion for the active site and allowing the diffusion of large molecules as polyaromatics [32,17,36–40].

In a previous work, we have shown that Ir-mesoporous catalysts have good performance in the hydrogenation of tetralin at mild conditions. We have found that the trans/cis decalin ratio remains constant with tetralin conversion. This behavior is different for a commercial NiMo catalyst, where the trans/cis ratio increases as the conversion increases [16]. We also obtained high yield to cis-decalin, which could be further opened to form products with a high cetane number in the Ring Opening reactions.

As we demonstrated that Iridium is selective for cis-decalin, and Platinum is very active for hydrogenation, here we prepared a bimetallic Ir–Pt-SBA-15 catalyst, with different proportion of each metal, in order to improve the hydrogenation of tetralin to cis-decalin. From a fundamental point of view, exploring bimetallic catalysts also allows better understanding of mechanisms and variables involved in the catalytic reactions. The features of the catalysts here studied are going to be correlated with their catalytic performance in the hydrogenation of tetralin under mild conditions in order to find the best yield to cis-decalin. The final goal is to find the optimal proportion of each metal in order to be more active and the best reaction conditions. The statistical experiments design is the process of planning an experiment to obtain appropriate data that can be analyzed by statistical methods, to produce concrete and valid conclusions [41–47]. One of the main advantages in the response curve is to visualize the response for all levels of the experimental factors. The objective is to select the levels of independent variables that optimize simultaneously all the responses. Experiment design-response surface methodology (RSM) is used in this work to model and optimize two responses (Conversion at 3 h and at 5 h or reaction time) in the process of hydrogenation of tetralin to decalin over bimetallic Ir–Pt-SBA15. In this study, a Box–Behnken design was applied in order to analyze the influence of the following factors: A: the Catalyst, B: the Relation mass of catalyst/mole of reagent and C: the Temperature of the reaction. The response surfaces find the best combination between the reaction parameters, which would allow optimizing the process.

2. Experimental

2.1. Synthesis of Si-SBA-15

Materials: Tetraethylorthosilicate (TEOS, 98%, Sigma–Aldrich), Poly(ethylene glycol)-block-poly(propylene glycol)-block-poly (ethylene glycol), (EO20PO70EO20, P123-Sigma–Aldrich). Ordered mesoporous silica SBA-15 was prepared by using the triblock copolymer, Poly(ethylene glycol)-block-poly(propylene glycol)-block-poly (ethylene glycol) as the surfactant and tetraethylorthosilicate as the silica source. The procedure designed is described as follows: 1.5 g of P123 was dissolved in a solution of HCl 2 M (48 mL) with stirring at 50 °C. Then, 3.7 mL of TEOS was added dropwise under stirring during 5 min. The resulting mixture was kept in a PP bottle under static conditions at 50 °C for 24 h. The milky mixture was aged at 80 °C for 72 h. The solid was filtered, washed with deionized water until pH ~6. The molar composition was 1TEOS:158H_2O:6HCl:1.6 × 10^{-2} P123. To extract the template, the material was first immersed in a solution of ethanol 50%v/v for 24 h. Then the product was filtered, washed, and dried in air at 50 °C. To ensure the elimination of the structure-directing agent, the sample was heated up to 470 °C, under a N_2 flow of 20 mL/min and then calcined at 500 °C in air for 5 h.

2.2. Synthesis of Ir–Pt-SBA-15

Platinum (Pt) and Iridium (Ir) nanoparticles were incorporated into SBA-15 support by the wet impregnation in the case of the monometallic and co-impregnation method for bimetallic catalysts. The metal precursors (Iridium acetylacetonate – ($Ir(acac)_2$) and chloroplatinic acid ($H_2PtCl_6xH_2O$)) were dissolved in 50 mL of ethanol at 50 °C under reflux, to have a nominal content of 1 wt.% of Ir and 0–1 wt.% of Pt in the final solid. A finely ground powder fraction of the SBA-15 was dried in static air at 120 °C for 12 h, then, it was directly incorporated to the platinum and iridium solution. The solution was placed in a rotary evaporator to remove excess of ethanol at about 50 °C and 60 rpm. The obtained powder was then dried at 120 °C overnight, and desorbed in inert atmosphere (nitrogen flow of 20 mL/min) from 25 °C to 470 °C with a slope of 4 °C/min and kept at 470 °C during 5 h. Then the samples were calcined at 500 °C for 5 h. Due to the metals being active for the reaction in its metallic state, the samples were reduced in H_2 flow of 20 mL/min at 470 °C using the same procedure described above. The total metal weight loadings were adjusted (from 0 wt.% to 2 wt.%) in order to have the desired metal molar fraction. Hereinafter these catalysts will be referred as: monometallic 1%Ir-SBA-15 and 1%

Please cite this article in press as: V.A. Valles, et al., Experimental design optimization of the tetralin hydrogenation over Ir–Pt-SBA-15, Catal. Today (2015), http://dx.doi.org/10.1016/j.cattod.2015.07.018

Pt-SBA-15, bimetallic 1%Ir–0.5%Pt-SBA-15, 1%Ir–0.75%Pt-SBA-15 and 1%Ir–1%Pt-SBA-15, where the molar fraction of iridium and platinum were 0.5Ir–0.5Pt, 0.6Ir–0.4Pt and 0.7Ir–0.3Pt, respectively.

2.3. Characterization of the catalysts

X-ray diffraction profiles of samples were recorded with aX'Pert Pro PANalytical diffractometer equipped with a CuKα radiation source (λ = 0.15418 nm) and X'Celerator detector based on Real Time Multiple Strip (RTMS). The samples were ground and placed on a stainless steel plate. The diffraction patterns were recorded in steps over a range of Bragg angles (2θ) between 0.4 and 6, at a scanning rate of 0.02 per step and an accumulation time of 20 s. Diffractograms were analyzed with the X'PertHighScore Plus software.

Elemental analysis was performed by inductively coupled plasma-atomic emission spectroscopy (VISTA-MPX) operated with high frequency emission power of 1.5 kW and plasma airflow of 12.0 L/min. The surface area was determined by the BET method using a Micromeritics Chemisorb 2720 apparatus, equipped with a TCD detector, after degassing the samples with N_2 (25 mL/min) at 400 °C.

X-ray Photoelectron Spectra (XPS) were obtained on a MicrotechMultilb 3000 spectrometer, equipped with a hemispherical electron analyzer and MgKα ($h\nu$ = 1253.6 eV) photon source. An estimated error of ±0.1 eV can be assumed for all measurements. Peak intensity was calculated from the respective peak areas after background subtraction and spectrum fitting by a combination of Gaussian/Lorentzian functions. Energy-dispersive X-ray analyses (EDX) were coupled to the scanning electron microscopy (SEM) LEO Mod. 440 equipment.

TEM were recorded in a JEOL 2100F microscope operated with an accelerating voltage of 200 kV (point resolution of 0.19 nm).

2.4. Catalytic activity

The catalytic activity was measured in a 4563 Parr reactor at 15 atm of hydrogen and 360 rpm at different temperatures. Feed consisted in 50 mL of tetralin (98.5% FLUKA) in dodecane, the amount of catalyst is set according to the ratio of mass catalyst/mole reagent corresponding to each reaction. The products were analyzed with a HP 5890 Series II GC and HP-5 column.

3. Results and discussion

3.1. Characterization of the catalysts

3.1.1. XRD

Low angle (0.4° < 2θ < 6°) X-ray diffraction patterns for SBA-15 support and for all Ir–Pt-SBA-15 catalysts are shown in Fig. 1. These materials display three well-resolved diffraction peaks

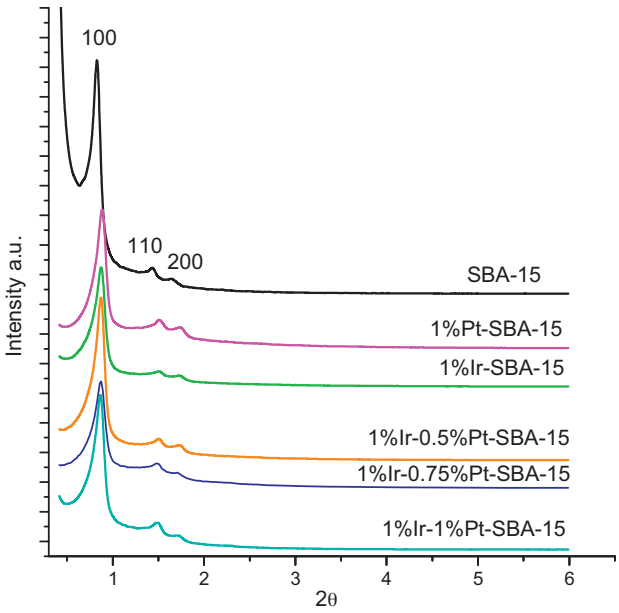

Fig. 1. XRD pattern of the synthesized samples.

characteristics of SBA-15. The most intense at 0.82° and two peaks with lower intensity at 1.43° and 1.64°, with Miller indexes (100), (110) and (200), respectively. These XRD profiles are characteristic of the two-dimensional p6mm hexagonal symmetry for parent SBA-15. When Pt and/or Ir are incorporated into the SBA-15 matrix, the peaks position slightly shifts to higher angles and the unit cell parameter (a_o) decreases (Table 1). However, the overall pore structure is retained as indicated by the appearance of low-angle diffraction peaks. The general decreasing in the intensity of diffraction peaks might be due to the reduction of scattering contrast induced by the dispersed nanoparticles [48,49].

3.1.2. TEM

The morphology of the support and dispersion of bimetallic nanoparticles over Ir–Pt-SBA-15 samples were examined by means of transmission electron microscopy (TEM). The TEM images of the catalysts and their corresponding PSDs (particle size distribution) are shown in Fig. 2. The particle size distribution ranging from 2 to 7 nm. A decrease of the Ir–Pt cluster dispersion and the consequent increase in the mean particle size when increasing the Pt loading was observed. The mean diameter of some of the Ir–Pt particles formed after calcination at 500 °C and reduction at 450 °C may exceeded the size of the SBA-15 cavities (8 nm) indicating that some of the clusters were located on the external surface of the SBA-15 crystallites. As we can see in Fig. 2, the mean particle diameter of 5 and 5.3 nm of 1%Ir–0.5%Pt-SBA-15 and 1%Ir–0.75%Pt-SBA-15, respectively, were found to be slightly smaller than the 6 nm of

Table 1
Physicochemical and structural properties of the catalysts.

Samples	a_0 (nm)	Area (m^2/g)	Ir, Pt (wt.%[a])	Crystal size (μm)[b]	V (mL/g)[c]	pD (nm)[c]	Cluster (size, nm[d,e])
SBA-15	12.37	1120	–, –	2.50	1.38	8.90	–, –
1%Ir-SBA-15	11.85	750	1.15, –	2.54	1.18	8.60	2.8, 3.2
1%Pt-SBA-15	11.84	700	–, 0.95	2.52	1.22	8.58	3.2, 3.5
1%Ir–0.5%Pt-SBA-15	11.83	689	1.12, 0.45	2.60	1.00	8.29	5.0, 5.4
1%Ir–0.75%Pt-SBA-15	11.83	668	1.21, 0.78	2.56	0.96	8.17	5.3, 5.4
1%Ir–1%Pt-SBA-15	11.80	650	1.11, 1.20	2.59	0.90	8.00	6.0, 6.2

[a] Data obtained by ICP.
[b] SEM.
[c] Average pore diameter (pD) and pore volume (V) determined from the adsorption isotherms by the BJH method.
[d] TEM of the fresh.
[e] TEM of the spent catalysts.

Please cite this article in press as: V.A. Valles, et al., Experimental design optimization of the tetralin hydrogenation over Ir–Pt-SBA-15, Catal. Today (2015), http://dx.doi.org/10.1016/j.cattod.2015.07.018

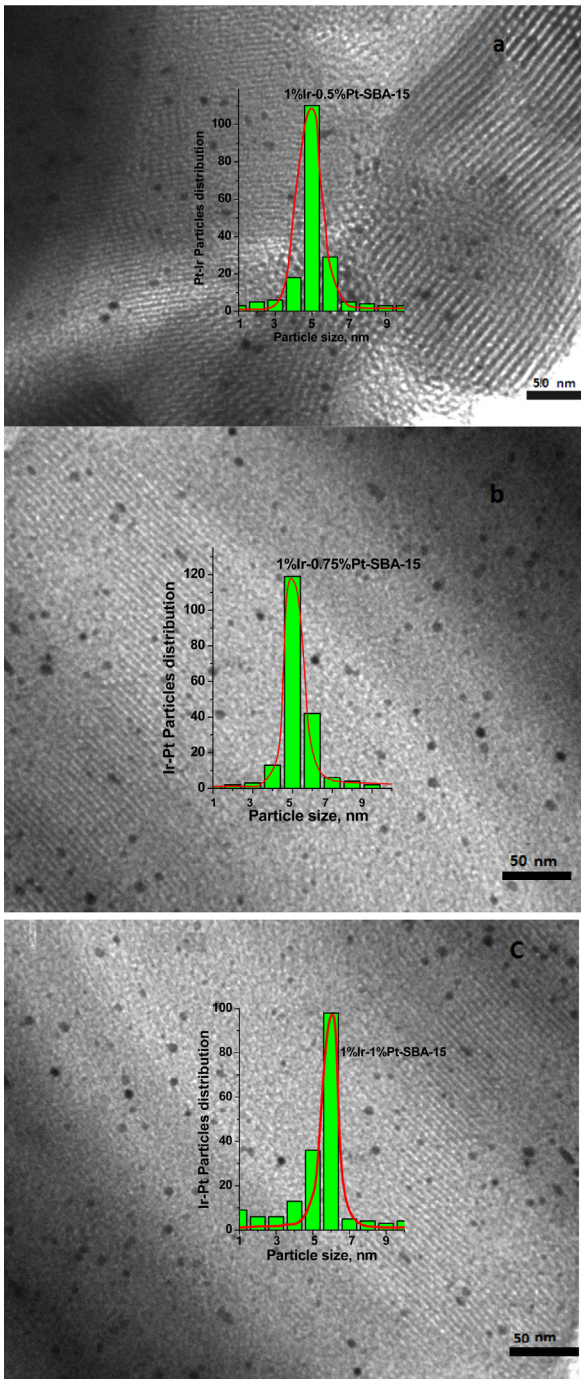

Fig. 2. TEM of the samples and particle size distribution. (a) 1%Ir–0. 5%Pt-SBA-15. (b) 1%Ir–0.75%Pt-SBA-15. (c) 1%Ir–1%Pt-SBA-15.

the sample with high metal loading 1%Ir–1%Pt-SBA-15. In addition, the samples with 0.5 and 0.75% Pt gave better dispersion of metal particles.

The textural and structural properties of Ir–Pt catalysts supported on SBA-15 materials are given in Table 1. The content of iridium and platinum in the catalysts was determined by ICP. The lower Ir–Pt cluster size was observed in 1%Ir–0.5%Pt-SBA-15 sample, with higher dispersion determined by TEM. The incorporation of a metal in the structure therefore leads to a slight decrease in the surface area but the pore diameter and the mesoporous character are maintained. After catalytic reaction with tetralin, the metal particle size estimated from TEM is unchanged.

Table 2
Contribution of Pt and Ir species (Pt^0, Pt^{2+}, Ir^0 and Ir^{2+}) in monometallic and bimetallic SBA-15 samples.

Samples	Pt^0, Pt^{2+} wt.% (*)	Ir^0, Ir^{2+} wt.% (*)
1%Ir–1%Pt-SBA-15	74, 26	68, 32
1%Ir–0.75%Pt-SBA-15	78, 22	88, 12
1%Ir–0.5%Pt-SBA-15	82, 18	91, 9
1%Pt-SBA-15	66, 34	–, –
1%Ir-SBA-15	–, –	89, 11

(*) From XPS studies, BE: Pt 4f7/2; Ir 4f7/2.

Rayo et al. [50] studied the effect on the structural stability of SBA-15 when the NiMo-SBA-15 catalytic materials were prepared under different pH conditions. The activity of the different catalysts evaluated in the thiophene hydrodesulfurization reaction was higher for the catalysts prepared at low pH. They demonstrated that the mesoporous structure of SBA-15 was preserved after the introduction of the different active sites at lower pH. In our case, Ir–Pt/SBA-15 material was obtained by incipient co-impregnation with Iridium acetylacetonate and chloroplatinic acid in absolute ethanol. The pH of the obtained solution was measured with a value close to 1.5. Even though, some polymerization of terminals silanols could be responsible for the observed reduction of area, the framework of silica SBA-15 is preserved after the treatment, in agreement with Rayo et al. [50].

3.1.3. XPS-SEM-EDX

The 4f signal of Ir or Pt nanoparticles dispersed in monometallic Ir–SBA-15 and Pt-SBA-15 are shown in Fig. 3a–b, and in bimetallic Ir–Pt-SBA-15 samples are shown in Fig. 3c–e. The Binding Energy (BE) of Pt4f of metallic Pt, in the metallic Pt-SBA-15 (Fig. 3a) appears at 71.1 eV, whereas in 1%Ir–1%Pt-SBA-15 (Fig. 3c) around 71.7 eV. Observe the shift to higher BE for Pt 4f in the Ir–Pt sample could be related to a lower electron density on the Pt sites due to the presence of Ir (higher electron affinity). In this way, a BE of Ir4f at 61.1 eV is observed in the Ir-SBA-15 sample (Fig. 3b), assigned to metallic iridium, while a small shift to lower BE (60.0–60.2 eV) is observed in the 1%Ir–1%Pt-SBA-15 sample (Fig. 3c). Both shifts of the BE of Ir and Pt suggest the formation of a bimetallic Ir–Pt alloy, as reported for similar systems following the Pt4f7/2 and Ir4f7/2 peaks [51–53]. This effect was found for all Ir–Pt-SBA-15 samples (Fig. 3c–e). On the other hand, the diminution of Ir–O species in Ir–Pt samples respect to Ir-SBA-15 indicated the electronic transfer from Pt to Ir. Table 2 shows the analysis of the contribution of Ir^0, Pt^0 and Ir^{2+} and Pt^{2+} in the samples according to the Figs. 3a–d.

From XPS analysis, Pt and Ir wt.% at 50–100 Å of depth were much lower than the data obtained by EDX analysis (Table 3), suggesting that the majority of Pt^0 and Ir^0 are within the nanostructure of SBA-15 samples.

3.2. Catalytic activity

In order to saturate aromatic hydrocarbons, conventional hydrotreating catalysts based on Co–Mo, Ni–Mo or Ni–W sulfides supported on alumina must work at severe operating conditions,

Table 3
Characteristics of Pt and Ir species obtained by XPS and EDX.

	Ir (wt.%)		Pt (wt.%)	
Sample	XPS	EDX	XPS	EDX
1%Ir–1%Pt-SBA-15	0.28	0.98	0.29	1.10
1%Ir–0.75%Pt-SBA-15	0.23	1.01	0.19	0.72
1%Ir–0.5%Pt-SBA-15	0.20	0.99	0.10	0.52
1%Ir-SBA-15	0.098	1.05	–	–
1%Pt-SBA-15	–	–	0.095	1.10

Please cite this article in press as: V.A. Valles, et al., Experimental design optimization of the tetralin hydrogenation over Ir–Pt-SBA-15, Catal. Today (2015), http://dx.doi.org/10.1016/j.cattod.2015.07.018

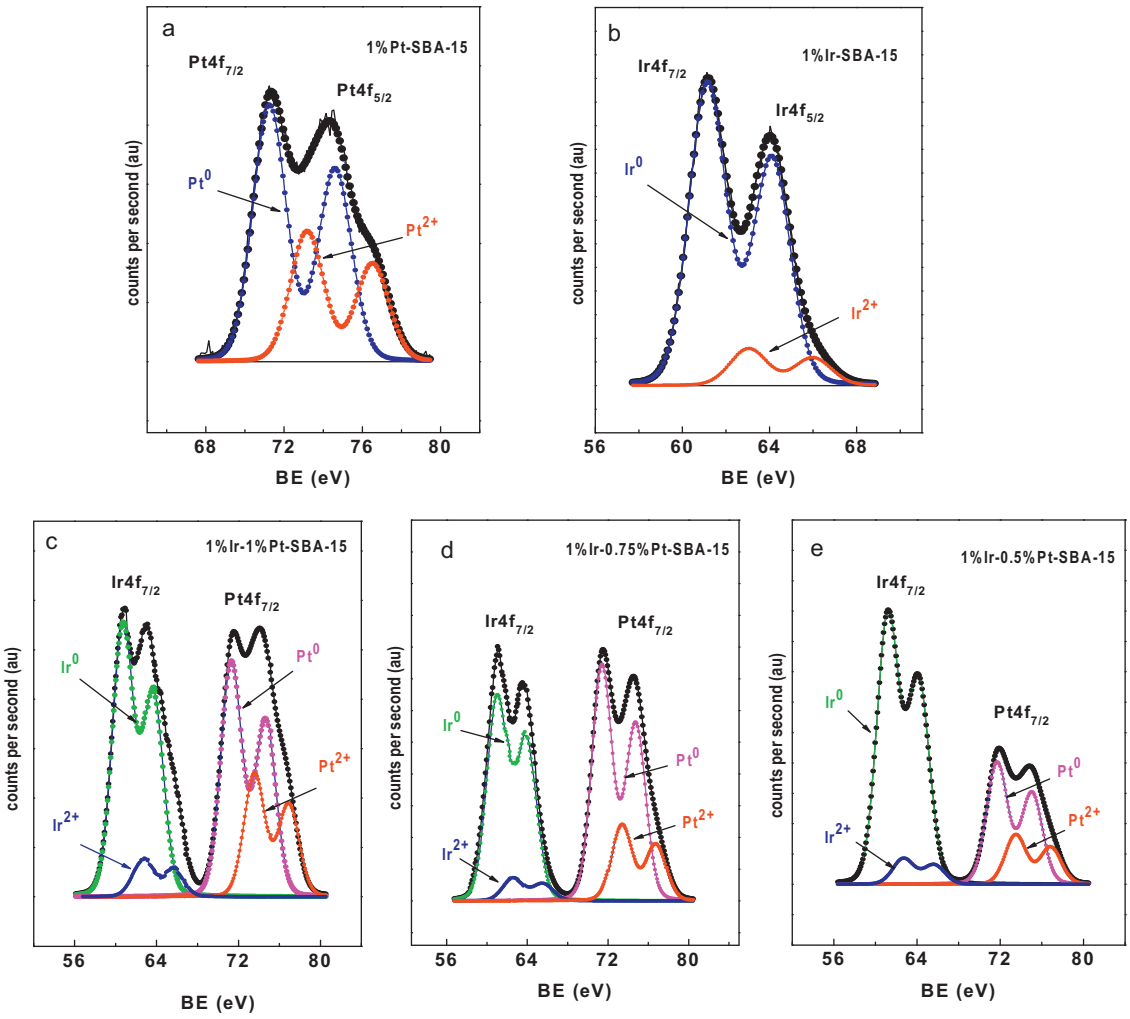

Fig. 3. XPS of 4f levels of Pt and Ir in: (a) 1%Pt-SBA-15, (b) 1%Ir-SBA-15, (c) 1%Ir–1%Pt-SBA-15, (d) 1%Ir–0.75%Pt-SBA-15 and (e) 1%Ir–0.5%Pt-SBA-15.

which increases the process cost. In this case, noble metal-based catalysts are an interesting alternative, since they have high activity for hydrogenation of aromatic hydrocarbons, and the process can then perform at lower temperatures and pressures and lower contact times. In previous works [14–16] we have investigated the best operation conditions for the hydrogenation of tetralin over several Iridium mesoporous materials. Different conditions were evaluated; at atmospheric pressure the catalyst exhibited dramatic decrease of the tetralin conversion values by increasing the reaction temperature, due to the thermodynamic constraints of the reaction. At 300 °C the fully hydrogenated products were not more detected, while, together with tetralin, traces of high-molecular-weight, ring-opening products and low-molecular-weight, cracking products were formed. We find the higher conversion when the tests were performed at 250 °C and 15 atm, while at higher pressures than 15 atm the catalytic activity slightly grew. In this work we set the pressure at 15 atm and temperature was varied in order to find the best activity. The major products in the hydrogenation of tetralin were trans-decalin and cis-decalin, naphthalene presence was negligible, due the experiments were performed far below the thermodynamic equilibrium. Decalins appeared to be unreactive under these conditions. The hydrocracking activity increases depending on the acidity of the support. In our case Si-SBA-15 was used as support, since no aluminum is present in the structure, the Bronsted acidity is very low and was not enough to lead to RO or hydrocracking products at the relatively low temperature of 200–250 °C. In agreement with this fact, Rayo et al. [54] studied the effect of the incorporation of Al, Ti, and Zr on the cracking and hydrodesulfurization activity of NiMo/SBA-15 catalysts at 400 °C and atmospheric pressure. The hydrocracking activity increased depending on the acidity of the support. They also found that acidity in the catalyst can come from the contribution of the support and/or from the presence of acid groups in the active (Mo or Ni) sulfide phases in the form of -SH groups. It appears then that the greater increase in HDS activity observed for the Al-containing catalyst, compared to those containing Zr or Ti, is related to the extra Brønsted acidity supplied by the support. Which are expected to enhance the hydrogenolysis step of the HDS reaction and help the transport of active hydrogen on the catalyst surface. Supporting this, Contreras et al. [55] studied the transformation of tetralin over a Pt catalyst supported on a hybrid material, HMFI–SBA-15. In at all the reaction temperatures, the main products were trans + cis-decalins. However, at high reaction temperature ring contraction to spirodecane and dehydrogenation to naphthalene were observed. At 325 °C, a maximum of 8% of ring contraction products was obtained. A reaction test using Pt/SBA-15 as reference was performed at 275 °C and 5.5 MPa of hydrogen pressure. The total tetralin conversion was 22% and the products were almost 100% cis + trans-decalin, no ring contraction or ring opening products were detected. In another work, Carrión et al. [56] studied the transformation of tetralin over PtPd/ZrMCM-41; their results indicated good hydrogenation with poor hydrogenolysis/ring opening

Please cite this article in press as: V.A. Valles, et al., Experimental design optimization of the tetralin hydrogenation over Ir–Pt-SBA-15, Catal. Today (2015), http://dx.doi.org/10.1016/j.cattod.2015.07.018

Table 4
The Box–Behnken design, showing the responses and the levels of the factors.

Factors			Response
A: Catalyst	B: Relation	C: Temperature	Conversion (3 h)
0.5	22.727	200	68.915
1	28.393	225	85.112
0.5	22.727	250	46.721
0.75	22.727	225	80.162

activity; showing that the acidity of Zr-modified MCM-41 was not enough to lead to RO products, although the authors reported the presence of some hydrocracking products.

Another interesting aspect of the present study is the analysis of the trans/cis selectivity in the decalin product. Weitkamp [57] explained the formation of cis- and trans decalins in terms of a intermediate Δ1,9-octalin (octa-hydro-naphthalene), which according to the author, is the most reactive octalin and, therefore, responsible for the formation of both decalin isomers. When the hydrogen atom in position 10 of this intermediate is oriented facing the surface, the hydrogenation of the double bond results in the formation of cis-decalin, because hydrogen addition to a double bond is always *syn* (both H atoms are added on the same side). By contrast, when the hydrogen atom in position 10 is oriented facing away from the surface, the *syn* hydrogenation addition results in the formation of trans-decalin. Accordingly, the trans/cis ratio would be determined by the preference of the intermediate to readsorb with the H in position 10 facing up or down, respectively. Alternatively, desorption of the Δ1,9-octalin may not be necessary for the formation of trans if it is considered that it may rollover on the surface and get hydrogenated on the opposite site [57,58]. One complication in analyzing the trans/cis selectivity is the decalin isomerization reaction, which greatly favors the formation of *trans* and also occurs on metals [59,60].

Experimental design will help us to find the best catalyst and the best operation conditions in the hydrogenation of tetralin and will also allow us to analyze the trans/cis selectivity.

3.3. Experimental design-response surface

In order to optimize the process of tetralin hydrogenation over Ir–Pt-SBA-15 at mild conditions, a Box–Behnken design was applied and the variables studied were: (A) nature of the catalyst (weight % of each metal on catalyst and total metal loading), (B) Relation: mass of catalyst/reagent moles and (C) reaction temperature, on two responses: conversion at 3 h and at 5 h of reaction time. We used the following levels:

(A) Catalyst: Iridium was set at 1 wt.% and Platinum varied from 0.5, 0.75 and 1 wt.%
(B) Relation: g cat/mol of tetralin were: 17, 22 and 28 g/mol
(C) Temperature: 200, 225 and 250 °C

Box–Behnken design has 15 experiments; the runs were randomly carried out and the data obtained were analyzed at the 95.0% confidence level. In the RSM, factorial design is performed, and the results are adjusted using mathematical models. These stages are known as displacement stage and design, respectively; they are repeated several times, screening the response surface obtained in the direction of the region of the best optimum point. The design was analyzed using Statgraphics and Statistica software®. Table 4 shows some relevant data of the design.

Table 5
Analysis of variance.

Source of variation	Sum of square	d.f.	Mean square	*F*-ratio	*p*-value
A: Catalyst	975.914	1	975.914	57.29	0.0006
B: Relation	19.823	1	19.823	1.16	0.3300
C: Temperature	86.527	1	86.527	5.08	0.0739
AB	111.714	1	111.714	6.56	0.0506
AC	405.217	1	405.217	23.79	0.0046
BC	4.247	1	4.247	0.25	0.6387
Total error	85.167	5	17.033		
Total (corr.)	2501.560	14			

R^2 = 96.5954%; R^2(adjusted for d.f.) = 90.4672%.

3.4. Response: conversion (3 h)

For each effect, the variance analysis (ANOVA) [61] partitions the variability of the response into separated pieces. ANOVA then, tests the statistical significance of each effect by comparing the mean square against an estimate of the experimental error.

The results obtained by the ANOVA test (Table 5) show, in this case, that the variables that influence significatively, on the Conversion with 95.0% of confidence level are: Catalyst and Catalyst–Temperature interaction and with 90.0% of confidence level, are: Temperature and Catalyst–Relation interaction.

The adjusted R-squared statistic [61] indicates that the model accounts for 90.47% of the variability found in Conversion (3 h). Here, this value indicates that the model explains 90.0% of the total variations.

According to the Pareto (Fig. 4), the parameters that produce a more pronounced effect on the Conversion are Catalyst and the interactions A–C at 95.0% and the interaction AB and Temperature at 90.0%. The positive sign in the effect of the factors suggests an increase in the response of the change from the lower to the higher level of the factor. The negative sign implies a decrease in the response of the change from the lower to the higher level of the factor. The contours of estimated response surface products of the design are shown in Fig. 5.

Fig. 5a shows the interaction between Relation (g cat/mol of tetralin) and Catalyst, in order to obtain the maximum Conversion we should working the dark red zone. Set Pt wt.% between 0.8 and 1.0 and the Relation between 17 and 18 g/mol or set Pt wt.% between 0.8 and 0.9 and Relation 27–28.

Fig. 5b shows the interaction between Temperature and Catalyst, in order to obtain the maximum Conversion we must set Pt wt.% between 0.7 and 0.8 and Temperature between 200 and 210 °C or set Pt wt.% between 0.9 and 1.0 and Temperature between 220 and 240 °C.

Fig. 5c shows the interaction between Temperature and Relation, this interaction is not significative (from the ANOVA test), but we can see that in order to obtain the maximum Conversion we should set Relation between 17 and 18 and temperature between 200 and 210 °C.

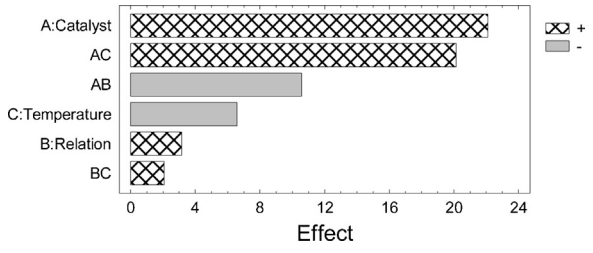

Fig. 4. Pareto chart.

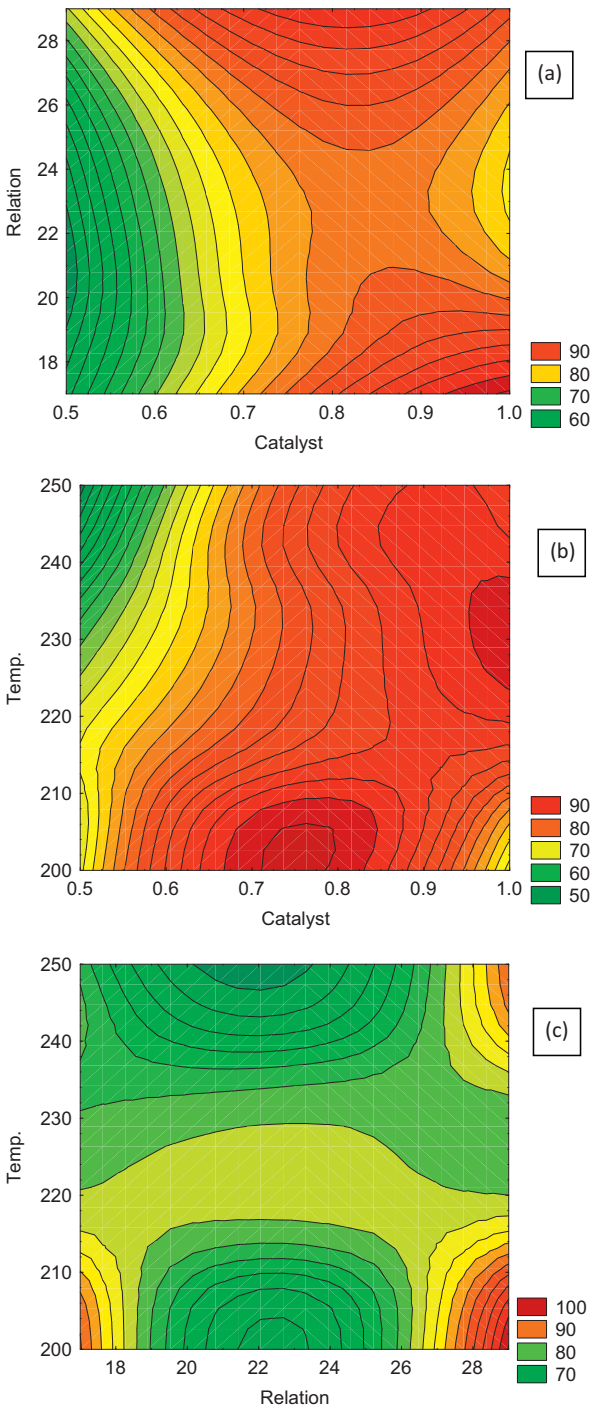

Fig. 5. Contour of response surface fitted for the design. Conversion (3 h) as a function of the (a) Relation and Catalyst, (b) Temperature and Catalyst and (c) Temperature and Relation.

3.5. Response: conversion (5 h)

In the case of the second response, Conversion at 5 h, the ANOVA test shows the variables that influence significatively on the Conversion are similar that at 3 h with 95.0% of confidence level are Catalyst, Temperature and Catalyst–Temperature interaction). The adjusted *R*-squared was 90.76%, this value indicates that the model explains 90% of the total variations. From the contour of response surface fitted for the design (not shown), we also can reach the same conclusions that at 3 h of reaction. With this fact, we can assume that a change in the time of reaction from 3 to 5 h, has no significant influence to change the results and conclusions obtained from the design.

The statistic methodology followed in this work, allows suggesting the better operation conditions for this reaction in order to optimize the Conversion.

We suggest the better operation conditions as follows:

Catalyst: 0.7–0.8 wt.% Pt
Relation: 17–19 g cat/mol TL
Temperature: 200–220 °C

The increase in Pt content to 1 wt.% fails to improve tetralin conversion. XPS analyses indicated that in the Pt-high loaded sample, a lower amount of reduced platinum was found than in the other samples. In addition, according to TEM, a decrease of the Ir–Pt clusters dispersion and the consequent increase in the mean particle size when increasing the Pt loading was observed. These could be the reasons why higher temperature and higher mass of catalyst per mol of tetralin is needed when wt.% Pt is increased to 1.

Results about the trans/cis selectivity are needed to address here, since cis-decalin at moderate temperatures is more selective to C10 ring-opening products [22]. To optimize the trans/cis ratio (minimum value) to attain high selectivity to cis-decalin a new Experimental Design should be done. In this work, we only find the optimal conditions for the tetralin conversion to decalins, but also we can provide an approach to find either, the better conditions to obtain higher yield to cis-decalin. To give an understanding of the whole process, we present the trans/cis decalin selectivity, using the contour plot, to show more clearly, how the trans/cis ratio is affected when the variables are varied simultaneously.

3.6. Trans/cis selectivity

To obtain a high selectivity to cis-decalin is an important goal in this work. The trans/cis ratio was found to be practically constant with the conversion for all the 15 experiments. In Fig. 6 we show the influence of the variables over the trans/cis selectivity. Fig. 6a shows the relationship between Temperature and Catalyst. We can observe here that with a low wt.% of platinum at any temperature we obtain a desired low trans/cis ratio (dark green zone) or in the case of a higher-loaded Pt catalyst we have to operate at lower temperatures or at high Relation (g cat/mol of TL) as can be seen in Fig. 6b. Fig. 6b also shows that with a low wt.% Pt close to 0.5 high selectivity to cis-decalin is reached at any relation. Fig. 6c shows that high yield of cis-decalin is reached at relation of 22 at low temperature or at relation of 28 at higher temperatures. Thus, Pt caused a significant increase to catalyst activity but the selectivity to the formation of cis decalin increases to at certain molar fraction and then decreases.

Fig. 7a shows that at high conversion (the values of conversion as response, were obtained at 3 h for the 15 experiments where the variables varied simultaneously) the trans/cis ratio is low for 0.5 wt.% Pt and Fig. 7b shows a low trans/cis ratio at lower temperatures and lower conversions. High trans/cis ratios obtained at elevated temperatures could be because cis-decalin is isomerized to trans-decalin, since trans-decalin is thermodynamically favored.

In resume, the trans/cis ratio decreases with decreasing of Pt molar fraction in the catalyst and decreasing of temperature and increases with lower relation mass of catalyst/mol of tetralin.

The trans/cis ratio obtained here for all the runs (between 0.3 and 0.6) is lower compared with that reported elsewhere for bimetallic system in a continuous flow reactor [18,19,17,55,62]. We already had obtained a lower trans/cis ratio, in a previous work using monometallic Iridium supported on titanium modified-SBA-16 [16].

Please cite this article in press as: V.A. Valles, et al., Experimental design optimization of the tetralin hydrogenation over Ir–Pt-SBA-15, Catal. Today (2015), http://dx.doi.org/10.1016/j.cattod.2015.07.018

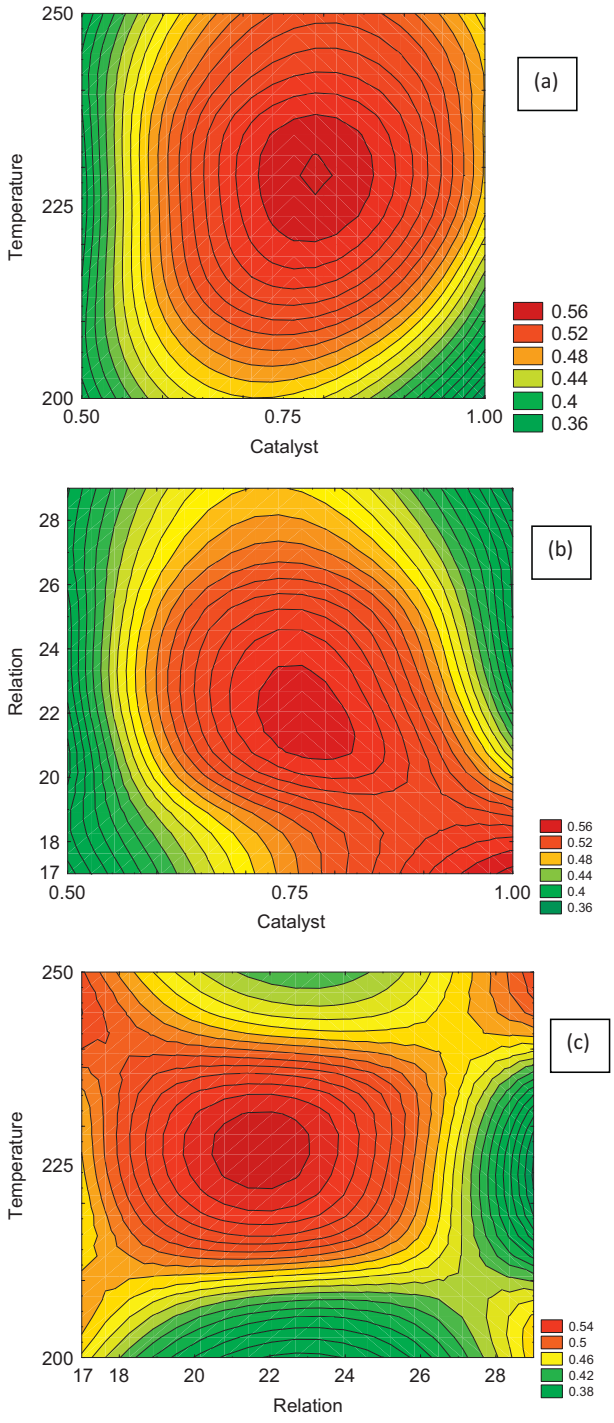

Fig. 6. Trans/cis selectivity as a function of the (a) Temperature and Catalyst, (b) Relation and Catalyst, and (c) Temperature and Relation. Note: This is not an Experimental Design Response. The trans/cis ratio was obtained for each run used in the design.

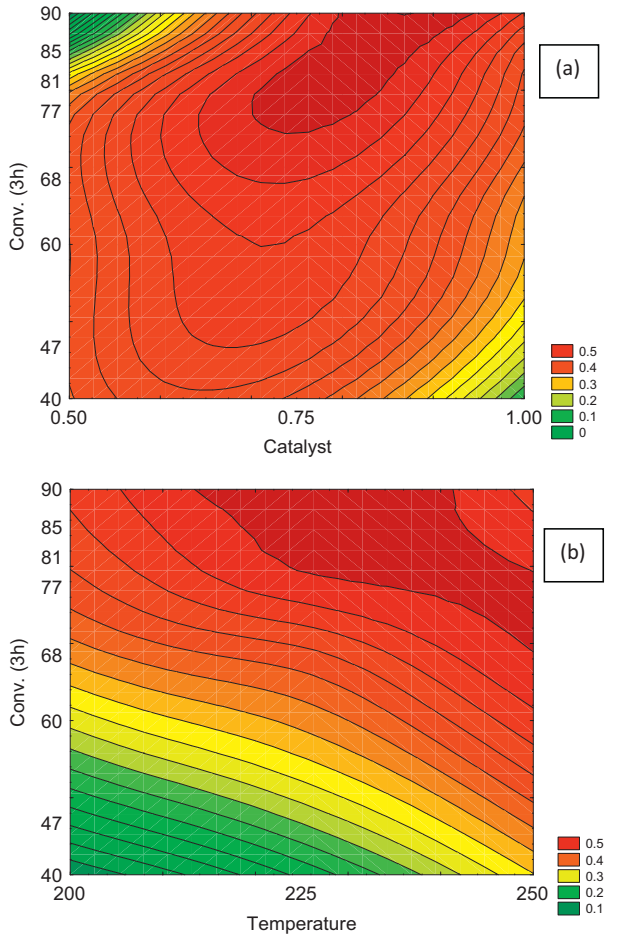

Fig. 7. Trans/cis selectivity as a function of the (a) Conversion and Catalyst (b) Conversion and Temperature. Note: This is not an Experimental Design Response. The trans/cis ratio was obtained for each run used in the design.

As were shown in literature, depending on the conversion level, the *cis–trans* isomerization can greatly affect the observed selectivity. We also observe that the trans/cis-decalin ratio is almost constant for all the catalyst tested in this study, similar results were obtained by Rocha et al. [19], where bimetallic Pt–Pd and Ir–Pd on Y zeolite showed a constant trans/cis ratio close to 2 vs. time on stream. They explain that the behavior with the cis/trans-decalin ratio is because coke deposition in the zeolite cavities impairs the desorption/re-adsorption mechanism responsible for trans-decalin formation and larger cis/trans ratios are observed with the catalysts containing more iridium. They associate this behavior to the strength of the bond between the intermediate that undergoes desorption/re adsorption and the metal. Iridium is a more hydrogenolysing metal than platinum and it deactivates more rapidly. Platinum bind hydrocarbon intermediates more loosely, this should facilitate the desorption/re-adsorption of the D1,9-octalin intermediate therefore favoring the formation of the trans isomer. Jongpatiwut et al. [62] explained the trans/cis ratio remained constant in terms of a strong competition for adsorption sites in which the cis-to-trans isomerization was blocked by adsorbed tetralin. Dokjampa et al. [18] concluded that in the case in which the hydrogen incorporation is fast, soon after the 1,9-octalin hits the surface it is hydrogenated. Therefore, one may expect a higher trans/cis ratio, as are the cases for Pt catalyst, which have high intrinsic hydrogenation activity. When the catalyst is much less active, as in the case of Pd, one may expect that 1,9-octalin may have time to accommodate and roll over on the surface before being hydrogenated to give trans decalin.

These could be the reasons why iridium is more selective to cis-decalin than platinum, and by using, a bimetallic Ir–Pt catalyst may have a catalyst where the intrinsic trans/cis ratio is inversely related to the hydrogenation activity; but further study on the mechanism of this reaction in a batch reactor is needed to highlight this fact.

The highest conversion and the best selectivity to cis-decalin was reached over:

Please cite this article in press as: V.A. Valles, et al., Experimental design optimization of the tetralin hydrogenation over Ir–Pt-SBA-15, Catal. Today (2015), http://dx.doi.org/10.1016/j.cattod.2015.07.018

Table 6
Conversion at 3 h in the optimal conditions.

Catalyst	Relation	Temperature	Conversion at 3 h	Trans/cis
0.7	17	210	89.25	0.45
0.8	19	210	91.83	0.50
0.9	18	220	92.71	0.56
0.8	18	200	95.01	0.40

Catalyst: 0.7–0.8 wt.% Pt
Relation: 17–19 g cat/mol TL
Temperature: 200–220 °C

To corroborate this, several reactions were performed in the optimal conditions. The results found in Table 6 show the optimal values of the reaction conditions, based on statistical analyses.

The best yield to cis-decalin of 74% was obtained with 1%Ir–0.8%Pt-SBA-15 at 200 °C and using 18 g cat/mol. This value is higher than any found in literature.

4. Conclusion

A design of experiment was carried out in order to study the influence of the variables on the Conversion. According to the statistic methodology applied in this work, the variable Catalyst has the best influence over the Conversion at the 95.0% confidence level and the better operation conditions for this reaction were found. The RSM allowed us to develop cost effective catalyst with optimal noble metal loading. High activity and a very high selectivity to cis-decalin were achieved at low temperature using a high surface area bimetallic catalyst.

Acknowledgments

The authors are very grateful to Drs. J.L. García Fierro, J.M Martin and H. Falcon for XPS and TEM characterization performed in ICP-CSIC, Madrid.

We thank CONICET Argentina, PIP CONICET 11220120100218CO (2013–2015), and MINCyT Cba 1210/07 (2007–2014) for financial assistance.

References

[1] M.D. Agee, S.E. Atkinson, T.D. Crocker, J.W. Williams, Non-separable pollution control: implications for a CO_2 emissions cap and trade system, 2012, http://dx.doi.org/10.2139/ssrn.2201652.
[2] China Climate Change Info-Net, Notice regarding promoting implementation schemes of a comprehensive energy reduction program in the twelfth five year plan issued by the State Council, 2011, http://www.ccchina.gov.cn/cn/NewsInfo.asp?NewsId=29448
[3] CLP China, CLP technology roadmap: transforming into a low-carbon energy portfolio, 2010, http://www.clpgroup.com//ourcompany/aboutus/resourcecorner./publications/pages/clptechnologyroadmap.aspx?lang=en
[4] Copenhagen Accord, China's Autonomous Domestic Mitigation Actions, UNFCCC, Bonn, Germany, 2010, http://unfccc.int/files/meetings/cop_15/copenhagen_accord/application/pdf/chinacphaccord_app2.pdf
[5] Environmental Protection Agency (EPA), National Emissions Inventory (NEI) Air Pollutant Emissions Trends Data, EPA, Washington, DC, 2012.
[6] A.C. Gurgel, S. Paltsev, J.M. Reilly, G. Metcalf, Environ. Dev. Econ. 16 (2011) 155.
[7] World Bank, World Development Indicators Online, World Bank, Washington, DC, 2012, http://publications.worldbank.org/WDI/
[8] M. Usman, D. Li, C. Li, S. Zhang, Sci. China Chem. 58 (2015) 738.
[9] M. Usman, D. Li, R. Razzaq, M. Yaseen, C. Li, S. Zhang, J. Ind. Eng. Chem. 23 (2015) 21.
[10] C. Stinner, R. Prins, T. Weber, J. Catal. 191 (2000) 438.
[11] G.B. McVicker, M.S. Touvelle, C.W. Hudson, D.E.W. Vaughan, M. Daage, S. Hantzer, D.P. Klein, E.S. Ellis, B.R. Cook, O.C. Feeley, J.E. Baumgartner, Exxon Research and Engineering Company, US Patent 5,763,731 (1998).
[12] S. Hantzer, D.P. Klein, E.S. Ellis, B.R. Cook, O.C. Feeley, J.E. Baumgartner, Exxon Research and Engineering Company US Patent 5,763,731 (1998).
[13] S. Hantzer, M.S. Touvelle, Chen, J. Exxon Research and Engineering Company, International Patent WO 97/09289 (1997).
[14] G. Balangero Bottazzi, M.L. Martínez, M. Gomez Costa, O. Anunziata, A. Beltramone, Appl. Catal. A: Gen. 404 (2011) 30.
[15] V. Valles, G. Balangero Bottazzi, M. Martínez, M. Gómez Costa, O. Anunziata, A. Beltramone, Ind. Eng. Chem. Res. 51 (2012) 7185.
[16] B.C. Ledesma, V.A. Valles, L.P. Rivoira, M.L. Martínez, O.A. Anunziata, A.R. Beltramone, Catal. Lett. 144 (2014) 783.
[17] Y. Yu, B. Fonfé, A. Jentys, G.L. Haller, J.A. Rob van Veen, O.Y. Gutiérrez, J.A. Lercher, J. Catal. 292 (2012) 13.
[18] S. Dokjampa, T. Rirksomboon, S. Osuwan, S. Jongpatiwut, D.E. Resasco, Catal. Today 123 (2007) 218.
[19] A.S. Rocha, E.L. Moreno, G.P.M. Da Silva, J.L. Zotin, A.C. Faro Jr., Catal. Today 133–135 (2008) 394.
[20] S. Nassreddine, L. Massin, M. Aouine, C. Geantet, L. Piccolo, J. Catal. 278 (2011) 253.
[21] L. Piccolo, S. Nassreddine, M. Aouine, C. Ulhaq, C. Geantet, J. Catal. 292 (2012) 173.
[22] M. Santikunaporn, J.E. Herrera, S. Jongpatiwut, D.E. Resasco, W.E. Alvarez, E.L. Sughrue, J. Catal. 228 (2004) 100.
[23] R. Moraes, K. Thomas, S. Thomas, S. Van Donk, G. Grasso, J.P. Gilson, M. Houalla, J. Catal. 299 (2013) 30.
[24] M.A. Vicericha, M. Oportusb, V.M. Beniteza, P. Reyes, C.L. Piecka, Appl. Catal. A: Gen. 480 (2014) 42.
[25] A.H. Alzaid, K.J. Smith, Appl. Catal. A: Gen. 450 (2013) 243.
[26] S.A. Kishore Kumar, M. John, S.M. Pai, Y. Niwate, B.L. Newalkar, Fuel Process. Technol. 128 (2014) 303.
[27] M.A. Arribas, P. Concepción, A. Martínez, Appl. Catal. A: Gen. 267 (2004) 111.
[28] K.C. Mouli, O. Choudhary, K. Soni, A.K. Dalai, Catal. Today 198 (2012) 69.
[29] D. Santia, T. Holla, V. Calemmab, J. Weitkampa, Appl. Catal. A: Gen. 455 (2013) 46.
[30] G.B. McVicker, M. Daage, M.S. Touvelle, C.W. Hudson, D.P. Klein, W.C. Baird, B.R. Cook, J.G. Chen, S. Hantzer, D.E.W. Vaughan, E.S. Ellis, O.C. Feely, J. Catal. 210 (2002) 137.
[31] M. Luo, Q. Wang, G. Li, X. Zhang, L. Wang, L. Han, Catal. Commun. 35 (2013) 6.
[32] K.K. Soni, K.C. Mouli, A.K. Dalai, J. Adjaye, Microporous Mesoporous Mater. 152 (2012) 224.
[33] K. Jaroszewska, A. Masalska, K. Bňaczkowska, J.R. Grzechowiak, Catal. Today 196 (2012) 110.
[34] J.C. Amezcua, L. Lizama, C. Salcedo, I. Puente, J.M. Dominguez, T. Klimova, Catal. Today 107–108 (2005) 578.
[35] R. Nava, R.A. Ortega, G. Alonso, C. Ornelas, B. Pawelec, J.L.G. Fierro, Catal. Today 127 (2007) 70.
[36] Y. Yu, B. Fonfé, A. Jentys, G.L. Haller, J.A. Rob van Veen, O.Y. Gutiérrez, J.A. Lercher, J. Catal. 292 (2012) 1.
[37] O. Gutierrez-Tinico, K. Romero-Moreno, E. Leocadio-Ceron, G. Fuentes-Zurita, T. Klimova, Rev. Mex. Ing. Quím. 5 (2006) 179.
[38] U. Nylen, J.F. Delgado, S. Järás, M. Boutonnet, Appl. Catal. A: Gen. 262 (2004) 189.
[39] Z. Vít, Appl. Catal. A: Gen, 322 (2007) 142.
[40] T. Klimova, O. Gutierrez, L. Lizama, J. Amezcua, Microporous Mesoporous Mater. 133 (2010) 91.
[41] G.E.P. Box, K.B. Wilson, J. R. Stat. Soc. Ser. B 13 (1951) 1.
[42] R.A. Fisher, The Design of Experiments, 2nd ed., Oliver and Boyd, Edinburgh and London, 1937, xi, 260 pp. 12s 6d.
[43] D.C. Montgomery, Design and Analysis of Experiments, 3rd ed., John Wiley & Sons, Inc, New York, 1991.
[44] S. Ferreira-Dias, A.C. Correia, F.O. Baptista, M.M.R. da Fonseca, J. Mol. Catal. B: Enzym. 11 (2001) 699.
[45] O.A. Anunziata, A.R. Beltramone, J. Cussa, Appl. Catal. A: Gen. 270 (2004) 77.
[46] G. Du, Y. Yang, W. Qiu, S. Lim, L. Pfefferle, G.L. Haller, Appl. Catal. A: Gen. 313 (2006) 1.
[47] M. Sen, H.S. Shan, Electro jet drilling using hybrid NNGA approach, Robot. Comput. Integr. Manuf. 23 (2007) 17–24.
[48] C. Liu, R. Tan, N. Yu, D. Yin, Microporous Mesoporous Mater. 131 (2010) 162.
[49] J.M. Juárez, M.B. Gómez Costa, O.A. Anunziata, Int. J. Energy Res. 39 (2015) 128.
[50] P. Rayo, M.S. Rana, J. Ramírez, J. Ancheyta, A. Aguilar-Elguézabal, Catal. Today 130 (2008) 283.
[51] T. Toda, H. Igarashi, H. Uchida, M. Watanabe, J. Electrochem. Soc. 146 (1999) 10.
[52] M. Wakisaka, S. Mitsui, Y. Hirose, K. Kawashima, H. Uchida, M. Watanabe, J. Phys. Chem. B 110 (2006) 46.
[53] I. Radev, G. Topalov, E. Lefterova, G. Ganske, U. Schnakenberg, G. Tsotridis, et al., Int. J. Hydrogen Energy 37 (2012) 9.
[54] P. Rayo, J. Ramírez, M.S. Rana, J. Ancheyta, A. Aguilar-Elguézabal, Ind. Eng. Chem. Res. 48 (2009) 1242.
[55] R. Contreras, J. Ramirez, R. Cuevas-Garcia, A. Gutierrez-Alejandre, P. Castillo-Villalon, G. Macias, I. Puente-Lee, Catal. Today 148 (2009) 49.
[56] M.C. Carrión, B.R. Manzano, F.A. Jalón, D. Eliche-Quesada, P. Maireles-Torres, E. Rodríguez-Castellón, A. Jiménez-López, Green Chem. 7 (2005) 793.
[57] A.W. Weitkamp, Adv. Catal. 18 (1968) 1.
[58] C.C. Costa Augusto, J.L. Zotin, A. da Costa Faro, Catal. Lett. 75 (2001) 37.
[59] L. Le Bihan, Y. Yoshimura, Fuel 81 (2002) 491.
[60] A.D. Schmitz, G. Bowers, C. Song, Catal. Today 31 (1996) 45.
[61] R.O. Kuehl, Design of Experiments, 2nd ed, Duxbury-Thomson Learning, Pacific Grove, 2000.
[62] S. Jongpatiwut, Z. Li, D.E. Resasco, W.E. Alvarez, E.L. Sughrue, G.W. Dodwell, Appl. Catal. A: Gen. 262 (2004) 241.

Please cite this article in press as: V.A. Valles, et al., Experimental design optimization of the tetralin hydrogenation over Ir–Pt-SBA-15, Catal. Today (2015), http://dx.doi.org/10.1016/j.cattod.2015.07.018